

# Journal of Materials Chemistry B

Accepted Manuscript



This is an *Accepted Manuscript*, which has been through the Royal Society of Chemistry peer review process and has been accepted for publication.

*Accepted Manuscripts* are published online shortly after acceptance, before technical editing, formatting and proof reading. Using this free service, authors can make their results available to the community, in citable form, before we publish the edited article. We will replace this *Accepted Manuscript* with the edited and formatted *Advance Article* as soon as it is available.

You can find more information about *Accepted Manuscripts* in the [Information for Authors](#).

Please note that technical editing may introduce minor changes to the text and/or graphics, which may alter content. The journal's standard [Terms & Conditions](#) and the [Ethical guidelines](#) still apply. In no event shall the Royal Society of Chemistry be held responsible for any errors or omissions in this *Accepted Manuscript* or any consequences arising from the use of any information it contains.



## RGDS covalently surfaced nanodiamond as tumor targeting carrier of VEGF-siRNA: Synthesis, characterization and bioassay

Chunying Cui,<sup>a</sup> Yaonan Wang,<sup>a</sup> Wen Zhao,<sup>a</sup> Kaikai Yang,<sup>a</sup> Xueyun Jiang,<sup>a</sup> Shan Li,<sup>a</sup> Ming Zhao,<sup>\*a,b</sup> Yuanbo Song,<sup>c</sup> Shiqi Peng<sup>\*a</sup>

Nonviral tumor targeting vector for siRNA transfer is of importance. Here, a novel delivery system consisted of covalent conjugate NDCO-RGDS and VEGF-siRNA, NDCO-RGDS/VEGF-siRNA, was presented. *In vitro* NDCO-RGDS/VEGF-siRNA released and transferred VEGF-siRNA in a long-acting manner. Comparing to control, NDCO-RGDS/VEGF-siRNA decreased the expression of VEGF mRNA and protein of HeLa cells by 88.41±3.49% and 83.94±2.00%, respectively. *In vivo* NDCO-RGDS/VEGF-siRNA exhibited gene silencing and slowed tumor growth. FT-MS spectrum analysis revealed that NDCO-RGDS/VEGF-siRNA mainly distributed in tumor tissue of the treated S180 mice. Therefore NDCO-RGDS could be considered a promising nonviral tumor-targeting vector for siRNA transfer in tumor therapy.

Received 00th January 20xx

Accepted 00th January 20xx

DOI:10.1039/x0xx00000x

www.rsc.org/MaterialsB

### Introduction

RNA interference (RNAi) is a post-transcriptional gene silencing phenomenon initiated by siRNA, and attracts more and more attention for the treatment of many genetic diseases in recent years.<sup>1</sup> siRNA is a 21-23 nt nucleotide double-stranded RNA molecule, participates into the RNA-induced silencing complex and induces the degradation of target mRNA.<sup>2</sup> siRNA rapidly becomes a useful tool to target several pathological conditions including cancer, autoimmune, infection and neuronal disease.<sup>3-5</sup> However, cell membrane prevents the crossing of the naked siRNA due to its negative-charge, water-solubility and high molecular weight.<sup>6,7</sup> Efficient carrier system is required to overcome these issues. Recently, more nanomaterials and nanotechnology have been developed for gene and protein therapy. The success of gene therapy strongly depends on gene delivery carrier system, which has the characteristics of lower toxicity, sustained, higher efficiency of transfection and higher efficiency of gene expression.<sup>3,7</sup> Among various nanomaterials, carbon-based

<sup>a</sup> School of Chemical Biology and Pharmaceutical Sciences, Capital Medical University; Beijing area major laboratory of peptide and small molecular drugs; Engineering Research Center of Endogenous Prophylactic of Ministry of Education of China; Beijing Laboratory of Biomedical Materials; Beijing 100069, China

<sup>b</sup> Faculty of Biomedical Science and Environmental Biology, Kaohsiung Medical University, Kaohsiung, Taiwan

<sup>c</sup> Guangxi Pusen Biotechnology Co. Ltd.

\*Authors to whom correspondence should be addressed. E-mails: sqpeng@bjmu.edu.cn, mingzhao@bjmu.edu.cn

nanomaterials, such as nanotubes, nanowire, graphene and nanodiamond (ND), attract much attention due to their remarkable physical, chemical and biological properties.<sup>7,8</sup> As a member of the carbon nanoparticles, ND has an increasing interest because of its biocompatibility and potential applications, and has been used to deliver drug, protein and gene.<sup>9,10</sup> ND's surface can be functionalized with carboxyl groups. The derivatives for specific or nonspecific binding nucleic acids and proteins can be applied in biomedicine.<sup>11</sup> Moreover, ND's have high ratio of surface area to volume, significant loading capacity and big functionalized surface, thereby can conjugate and absorb a variety of small molecules.<sup>10-12</sup> The delivery consisted of antitumor agents such as 10-hydroxy-camptothecin and ND, a non-covalently bound delivery carrier,<sup>13</sup> and the delivery consisted of proteins such as bovine insulin and ND, a pH-dependent carrier,<sup>14</sup> were reported. For delivering siRNA ND and hydroxylated ND have many advantages such as low toxicity, biodegradability and absorbability.<sup>12,13,15</sup> Hydrogenated cationic ND was reported having high ability of loading and delivering siRNA into cells.<sup>16</sup> The gene of green fluorescent protein was also transferred into the nuclei of HeLa cells by ND.<sup>17</sup> RGDS can target tumor cell,<sup>18</sup> and the ND absorbed RGDS (ND/RGDS) can efficiently deliver siRNA into HeLa cells and block the expression of VEGF in our previous work.<sup>19</sup> However leaking RGDS from ND/RGDS remains to be solved. In this context here we report RGDS covalently functionalized ND (NDCO-RGDS) as tumor targeting carrier of VEGF-siRNA.

## Materials and Methods

### Materials

ND with an average particle size less than 10 nm and Arg-Gly-Asp-Ser (RGDS) were purchased from Sigma-Aldrich (USA). Anti-VEGF siRNA and fluorescein-labeled VEGF-siRNA (FAM-VEGF-siRNA) were purchased from GenePharma Co., Ltd (Shanghai, China). Dulbecco's modified Eagle medium (DMEM), fetal bovine serum (FBS) and trypsin were purchased from Hyclone Laboratories Inc (USA). Penicillin and streptomycin were purchased from Sigma Chemical Company (USA). Dimethyl sulfoxide (DMSO) was purchased from AppliChem GmbH Company (Germany). 3-(4,5-Dimethyl-thiazol-2-yl)-2,5-diphenyltetrazoliumbromide (MTT, Sigma, USA) and acridine orange were purchased from Amresco company (USA). Protease inhibitor cocktail (1%, Cat No: 539134) was purchased from Merck (USA). Primary antibodies against VEGF were purchased from Santa Cruz (Santa Cruz Biotechnology, USA). BCA protein kit was purchased from Pierce (Rockford, USA). Anti-mouse and anti-rabbit secondary antibodies were purchased from Amersham Life Science (USA). Matrigel was purchased from BD Bio-sciences (USA). All reagents were chemical grade unless otherwise specified.

### Preparation of NDCO-RGDS/VEGF-siRNA

RGDS covalently functionalized ND, NDCO-RGDS, and NDCO-RGDS/VEGF-siRNA were prepared by using the 5-step procedure depicted in Scheme 1.

### Preparation of NDCO<sub>2</sub>H

Following the procedure of the literature, the surface of ND was firstly functionalized with carboxyl group.<sup>17-20</sup> Briefly, 0.5 g of ND was oxidized in 10 mL mixture of concentrated H<sub>2</sub>SO<sub>4</sub> and HClO<sub>3</sub> (v/v, 3/1) at 40°C for 24 h, the reaction mixture was centrifuged (Centrifuges 5810R, Eppendorf, Germany) at 5000 g for 5 min, the supernatant was moved, the precipitates were suspended in 20 mL aqueous solution of NaOH (0.1 M), the suspension was stirred at 90°C for 1 h, and centrifuged at 5000 g for 5 min. The precipitates were suspended in 20 mL of hydrochloric acid (0.1 M), stirred at 90°C for 1 h and washed with deionized water for 3 times. NDCO<sub>2</sub>H were collected by centrifugation at 13000 g for 30 min, rinsed with deionized water for 3 times until neutral pH was achieved, and then was lyophilized.

### Preparation of NDCOCl

To promote the coupling of NDCO<sub>2</sub>H and RGDS, 59 mg of NDCO<sub>2</sub>H were converted into more reactive NDCOCl by using 10 mL of thionyl chloride.<sup>20-22</sup> The mixture was ultrasonicated at a frequency of 25 kHz in a bath sonicator for 1 h, filtrated for 0.5 h at room temperature, and dried overnight under high vacuum.

### Preparation of Arg(NO<sub>2</sub>)-Gly-Asp(OBzl)-Ser(Bzl)-OBzl

A solution of 30 mg of Boc-Arg(NO<sub>2</sub>)-Gly-Asp(OBzl)-Ser(Bzl)-OBzl in 6 mL of TFA was stirred at room

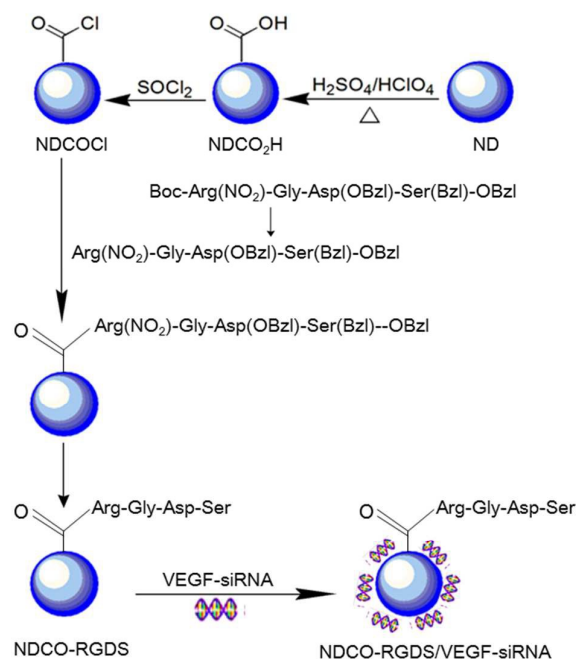
temperature for 30 min. The reaction mixture was evaporated at room temperature to move excess TFA, the residue was suspended in 10 mL of anhydrous ether, centrifuged at 8000 g for 10 min, the collected precipitates were suspended in 10 mL of anhydrous ether and centrifuged at 8000 g for 10 min to collect the precipitates of Arg(NO<sub>2</sub>)-Gly-Asp(OBzl)-Ser(Bzl)-OBzl.

### Preparation of NDCO-Arg(NO<sub>2</sub>)-Gly-Asp(OBzl)-Ser(Bzl)-OBzl

A solution of 15 mg of Arg(NO<sub>2</sub>)-Gly-Asp(OBzl)-Ser(Bzl)-OBzl in 10 mL of DMF and 60 mg of NDCOCl were suspended in 5 mL of DMF. The suspension was stirred at 75°C for 45 min, ultrasonicated for 72 h, and lyophilized to provide the title compound.

### Preparation of NDCO-RGDS

The removal of OBzl and NO<sub>2</sub> was achieved in 10 mL of ethanol by using Pd/C and hydrogen. After filtration, the powders were dried overnight under high vacuum to provide NDCO-RGDS.<sup>17,20</sup> Weight loss method was used to calculate the amount of RGDS. Formula:  $W_{(RGDS)} = W_{(NDCO-RGDS)} - W_{(NDCOOH)} - W_{(H_2O)}$ . It was found that 9.57 μg of RGDS was linked to 1 mg of ND.



Scheme 1 Synthetic route to preparing NDCO-RGDS/VEGF-siRNA.

### siRNA and VEGF-siRNA

A scramble sequence siRNA served as control. The VEGF-siRNA sequences of sense and anti-sense were 5'-GGAGUACCCUG-AUGAGAUCdTdT-3' and 5'-GAUCUCAUCAG-GGUACUCCdTdT-3', respectively.

### Preparation of NDCO-RGDS/VEGF-siRNA

The nanoparticle was induced by adding NDCO-RGDS to VEGF-siRNA solution with a gentle shaking and incubated 30 min at room temperature. All nanoparticles were induced in DEPC water and freshly prepared before use.

#### Characteristics of NDCO-RGDS/VEGF-siRNA

The sizes and  $\zeta$ -potentials of NDCO-RGDS/VEGF-siRNA were measured by a Zetasizer Nano ZS (Malvern Instruments Ltd., Malvern, UK) at room temperature. From 200  $\mu\text{g}$  of NDCO-RGDS/VEGF-siRNA the concentration of VEGF-siRNA was found to be 100 nM. The samples were measured in triplicate.

The nano-image of NDCO-RGDS/VEGF-siRNA (VEGF-siRNA, 100 nM) was observed on Scanning Electron Microscope (SEM, HITACHI S-4800, Japan).

Shape examinations of NDCO-RGDS were performed with transmission electron microscopy (TEM) (JSM-6360 LV, JEOL, Tokyo, Japan). An aqueous solution of nanoparticle was dripped onto a copper grid, and then a drop of a hydrous ethanol was added to promote water removal. The grid was first allowed to dry thoroughly in air and it was then heated at 35°C for 24 hours. The TEM was operated at 80 kV of the electron beam accelerating voltage. Images were recorded on an imaging plate (Gatan Bioscan Camera model 1792) at 6000-400000 $\times$  and were digitally enlarged.

Atomic force microscopy (AFM) images were obtained using the contact mode on Nanoscope 3D AFM (Veeco Instruments, Inc., Plainview, NY, USA) under ambient conditions. Samples in mouse plasma ( $10^{-6}$  M at pH 7.0) were used for recording the images.

The nano-property and opalescent light of NDCO-RGDS in aqueous solution was visualized with laser (650 nm), which induced Faraday-Tyndall effect. 25  $\mu\text{g}/\text{mL}$  and 50  $\mu\text{g}/\text{mL}$  of NDCO-RGDS in ultrapure water were irradiated with laser beam of 650 nm, respectively, as well as laser beam induces no Faraday-Tyndall effect in ultrapure water irradiated with laser beam of 650 nm.

The IR spectra of ND, NDCO-RGDS and NDCO-RGDS/VEGF-siRNA were observed by FTIR spectra (IR Prestige-21, Japan).

#### Cell culture

HeLa cells were cultured to 70-80% confluence in DMEM medium containing 10% fetal bovine serum, L-glutamine (2 mM), penicillin (100 U/mL) and streptomycin (100  $\mu\text{g}/\text{mL}$ ). Cells were cultured in an incubator at 37 °C in 5% CO<sub>2</sub> atmosphere. The cells were seeded into 24-well plates at a density of  $1 \times 10^5$  cells/well containing the culture medium and incubated prior to transfection experiments.

#### Calorimetric analysis of NDCO-RGDS absorbing VEGF-siRNA

Calorimetric analysis was carried out using differential scanning calorimetry (DSC, Netzsch, Germany) in a nitrogen atmosphere to determine the absorption of VEGF-siRNA onto NDCO-RGDS. In brief 400  $\mu\text{g}$  of NDCO-RGDS/VEGF-

siRNA (final concentrations of siRNA: 0, 20, 40, 60, 80 and 100 nM) were placed in a pierced aluminum pan, heated from 20°C to 200°C at a rate of 20°C/min (heating scan), kept at 200°C for 1 min to eliminate thermal history, and then cooled to 20°C at a rate of -40°C/min (cooling scan). The DSC curves were recorded by triplicates.

#### *In vitro* release of VEGF-siRNA from NDCO-RGDS/VEGF-siRNA

Dilutions of 2.0 mg of NDCO-RGDS/VEGF-siRNA ( $759 \pm 82$  ng/mg,  $1167 \pm 36$  ng/mg,  $1928 \pm 116$  ng/mg) in DEPC were suspended in 0.5 mL of TE buffer [Tris-HCl (10 mM) and EDTA (1 mM), pH 8.0] in RNase-free tubes and shaken in a water bath at 37°C. The supernatant was periodically collected at the given time points, and centrifuged (15000 g for 15 min). The released VEGF-siRNA was measured using a Victor X5 (PE, USA) plate reader at an excitation wavelength of 492 nm and emission wavelength of 520 nm. The percentage of cumulatively released VEGF-siRNA was calculated based on the standard curve of VEGF-siRNA. All experiments were repeated for five times.

#### Real-Time PCR

The transfection of VEGF mRNA towards HeLa cells was analyzed by RT-PCR.<sup>23</sup> HeLa cells were transfected by NDCO-RGDS/VEGF-siRNA (final concentration of siRNA, 100 nM) for 48 h and then harvested. VEGF mRNA in the transfected cells was compared with that in vehicle, NC, 100 nM naked VEGF-siRNA, NC/Lipo<sup>TM</sup>2000, NC/NDCO-RGDS and VEGF-siRNA/ Lipo<sup>TM</sup>2000. The total RNA was isolated using Trizol reagent (Invitrogen, USA), and RT-PCR was performed according to standard instructions (Real-time PCR System, model 7500, Applied Biosystems, Carlsbad, CA, USA). The cycling procedure consisted of an initial denaturation step for 10 min at 95°C followed by 40 cycles of denaturation at 95°C for 15 s, and annealing at 60°C for 1 min. Each sample was also subjected to melting curve analysis to confirm amplification specificity. Samples were run in triplicate, and each experiment included two non-template control wells. Samples were normalized to glyceraldehyde 3-phosphate dehydrogenase (GAPDH), and expressed as relative expression using the delta-delta Ct method. Results are represented as average  $\pm$  SD. The average threshold cycle (Ct) was automatically calculated using Applied Biosystems Sequence detection software (7500 Fast System SDS Software version 1.4). The primers to detect VEGF were as follows: Forward sequence: 5'-ATCGAGACCCTGGTGGACA-3', reverse sequence: 5'-CCGCCTCGGCTTGTGTCACA-3' and for GAPDH were: Forward sequence: 5'-CAAATTCCATGGCACCGTCA-3', reverse sequence: 5'-GGAGTGGGTGTCGCTGTTGA-3' and were synthesized and purified by GenePharma Co., Ltd (Shanghai, China).

#### ELISA to detect VEGF *in vitro*

The day before transfection,  $5 \times 10^4/\text{mL}$  HeLa cells were seeded in 24-well plates. When the cells were 70-80% confluent, they were washed with PBS for three times, and then transfected with vehicle, NC, VEGF-siRNA,

NC/Lipo<sup>TM</sup>2000, NC/NDCO-RGDS, NDCO-RGDS/VEGF-siRNA or VEGF-siRNA/Lipo<sup>TM</sup>2000 in Opti-MEM medium for 20 min. The cells were cultured at 37°C for another 48 h in a humidified 5% CO<sub>2</sub> atmosphere. The supernatants were collected and the amount of VEGF was measured using a VEGF ELISA kit (R&D, USA) according to the instructions. The untransfected cells were treated by the same method as a control to provide a baseline level of VEGF. Plates were read at 450 nm using a Victor X5 (PE, USA) reader. All experiments were repeated six times.

#### Cytotoxicity assay

HeLa cells were used for cytotoxicity assay. The cells were seeded in 96-well plates at a density of  $5 \times 10^3$  cells/well and incubated overnight at 37°C. The medium was replaced with vehicle, NC, VEGF-siRNA, NC/Lipo<sup>TM</sup>2000, NC/NDCO-RGDS, NDCO-RGDS/VEGF-siRNA or VEGF-siRNA/Lipo<sup>TM</sup>2000 and the cells were cultured for 72 h. MTT stock solution was prepared at a concentration of 2 mg/mL in cell medium and filter sterilized. Upon removal of the medium, MTT solution was added (50  $\mu$ L/well) and incubated in the dark at 37°C for 4 h. The MTT solution was removed and the dye was dissolved in DMSO (50  $\mu$ L/well) with agitation. The absorbance was measured at 570 nm and the IC<sub>50</sub> was determined. All experiments were repeated five times.

#### Confocal image of NDCO-RGDS/VEGF-siRNA treated HeLa cells

Intracellular location of NDCO-RGDS/VEGF-siRNA was investigated by confocal laserscanning microscopy (LEICA TCS SP5, Germany). HeLa cells were cultured in 35 mm glass bottom culture dishes for 24 h. The media were replaced with 1 mL of the media, VEGF-siRNA (100 nM) or NDCO-RGDS/VEGF-siRNA (100 nM). After incubation at 37°C for 6 h, the culture media were removed and the cells were rinsed with ice PBS for 3 times. The cells were fixed with 4% paraformaldehyde for 20 min, and DAPI (final working concentration 10  $\mu$ g/mL) was added to stain the cell nuclei for 10 min before the imaging. Intracellular location of VEGF-siRNA was observed using a confocal microscope excited at 358 nm and 461 nm, and emitted at 488 nm and 518 nm for DAPI and FAM, respectively. The images were analyzed using Leica CLSM software.

#### In vivo NDCO-RGDS/VEGF-siRNA inhibiting tumor growth

Male ICR mice (six-week-old, 18-22 g) were from Animal Department of Capital Medical University (Beijing Laboratory Animal Center, Beijing, China), and housed in an air-conditioned room. All care and handling of animals were approved by Institutional Authority for Laboratory Animal Care of Capital Medical University. S180 cells were gained from Vital River Laboratory Animal Technology Co., Ltd. Beijing, China, and xenografted subcutaneously in male ICR mice. The mice were housed in sterile isolated cages at

constant temperatures (22-25 °C) and free access to food and water. Tumor growth was monitored by measuring the tumors perpendicular diameter using a caliper. Tumor volume was calculated through the formula: volume (mm<sup>3</sup>) = length  $\times$  width<sup>2</sup> / 2.

After seven days the average volume of tumors xenograft reached 70-80 mm<sup>3</sup>, the mice xenografted S180 tumors were randomly divided into three groups (n=10), intravenously injected with NDCO-RGDS/VEGF-siRNA nanoparticles at a siRNA dose of 0.3 mg/kg and a NDCO-RGDS dose of 0.2 mg/kg in 0.2 mL volume at every other day for a total of 5 times, while the mice intravenously injected with normal saline and naked VEGF-siRNA (0.3 mg/kg) were used as the controls. On the day after the last injection, the tumors were harvested from the tumor-bearing mice for the tumor growth suppression tests. The brain, liver, spleen, lung, heart, kidney and tumor were homogenized on the ice, and washed with distilled water for three times to extract RGDS. The samples were centrifuged, collected the supernatant, and lyophilized. The existence of RGDS was analysed with FT-MS spectra.

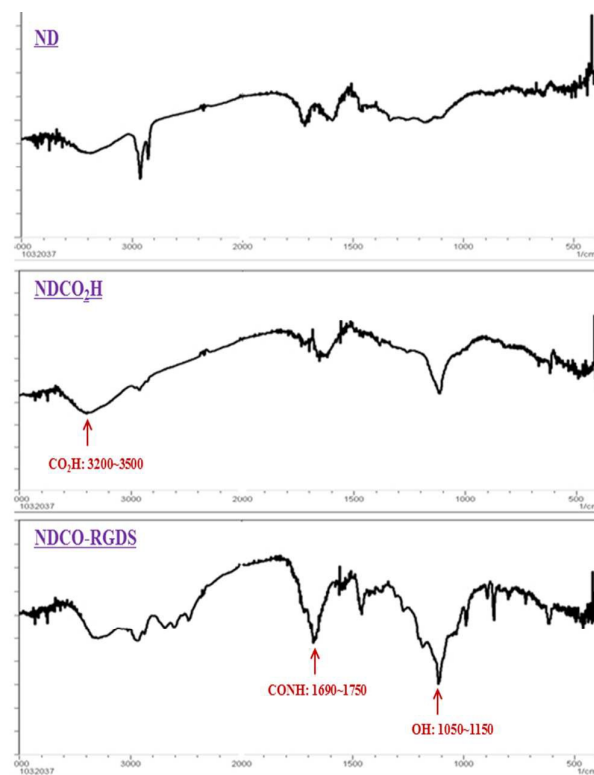


Fig. 1 FT-IR spectra of ND, NDCO<sub>2</sub>H and NDCO-RGDS.

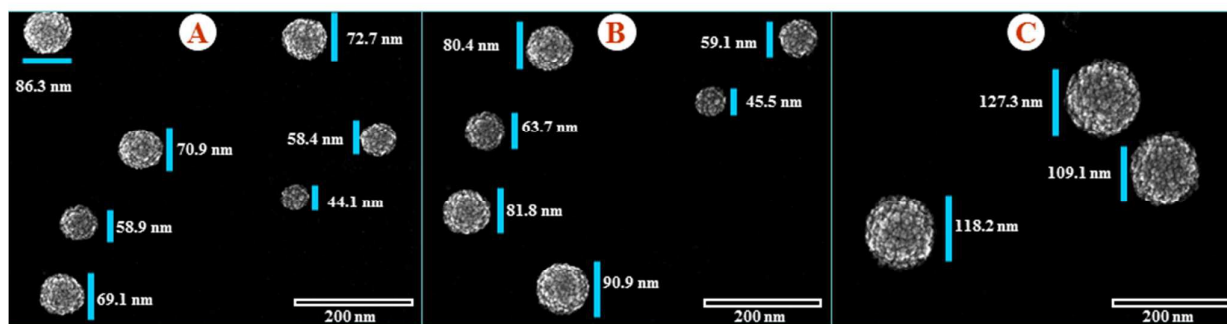


Fig. 2 (A) SEM image of NDCO<sub>2</sub>H; (B) SEM image of NDCO-RGDS; (C) SEM image of NDCO-RGDS/VEGF-siRNA.

### Statistics

All experiments were performed for at least three times. Data are represented as the average  $\pm$ SD. Paired two-sample Student's *t*-test was used for statistical analysis. A *p*-value of  $<0.05$  was considered statistically significant, and a *p*-value  $<0.01$  was considered very significant.

## Results and discussion

### SEM, FT-IR, TEM, AFM, and Tyndall effect

The FT-IR spectra of ND, NDCO<sub>2</sub>H and NDCO-RGDS are shown in Fig. 1. The FT-IR spectrum of NDCO<sub>2</sub>H shows a broad peak of CO<sub>2</sub>H groups at 3200-3500 cm<sup>-1</sup>. Comparing with the FT-IR spectrum of NDCO<sub>2</sub>H, the spectrum of NDCO-RGDS shows a broad peak of CO<sub>2</sub>H groups at 3200-3500 cm<sup>-1</sup>, the peak of CH at  $\sim$ 2900 cm<sup>-1</sup>, the peak of the carbonyl groups of the amide at  $\sim$ 1690 cm<sup>-1</sup>, and the peak of C-N at  $\sim$ 1150 cm<sup>-1</sup>, suggesting RGDS was covalently coupled with the CO<sub>2</sub>H groups successfully. The covalent modification of NDCO<sub>2</sub>H with RGDS was evidenced by FT-IR spectra.<sup>20,21</sup> In contrast to NDCO<sub>2</sub>H, NDCO-RGDS gives additional peaks at 1690-1750 cm<sup>-1</sup> and 1050-1150 cm<sup>-1</sup>, which are resulted from the covalently coupled RGDS.

The nano-structures were characterized with SEM image. Fig. 2 indicates that NDCO<sub>2</sub>H forms nano-particles of 44.1-86.3 nm in diameter, while NDCO-RGDS and NDCO-RGDS/VEGF-siRNA consistently form nano-particles of 44.1-127.3 nm in diameter. Regarding the zeta potential, NDCO<sub>2</sub>H, NDCO-RGDS and NDCO-RGDS/VEGF-siRNA have the positive values of  $13.4 \pm 4.2$  mV,  $28.4 \pm 3.8$  mV and  $25.4 \pm 6.4$  mV, respectively. The biocompatibility and the cellular uptake of the nano-particles depend on the surface characteristics, size, shape and aggregation.<sup>17,28,29</sup> Two hours after the incubation the nano-particles with an average sizes of  $\sim$ 50 nm can be delivered into HeLa cells by clathrin-mediated endocytosis, and after modifications the size could be slightly increased.<sup>21,22</sup> Four hours after the incubation the nanoparticles with an average size of 100 nm can be delivered into cancer and stem cells via macropinocytosis. NDCO-RGDS/VEGF-siRNA forming the nanoparticles of 109-127

nm in diameter suggests via macropinocytosis they can enter cancer cells.

The nano-structures were also characterized with the TEM images. Fig. 3 indicates that in ultrapure water (pH 7.4) 25  $\mu$ g/mL and 50  $\mu$ g/mL of NDCO-RGDS form the nano-particles of 29-89 nm and 39-85 nm in diameter, respectively, suggesting the concentration does not significantly affect the nano-size.

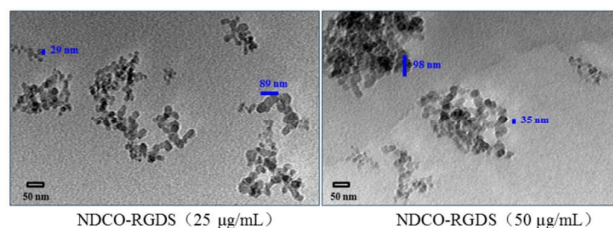


Fig. 3. Effects of 25  $\mu$ g/mL and 50  $\mu$ g/mL of NDCO-RGDS on TEM images.

The nano-structures were further characterized with the AFM images. Fig. 4 indicates that in blood 25  $\mu$ g/mL and 50  $\mu$ g/mL of NDCO-RGDS forms the nanoparticles of  $\sim$ 90.022 nm and  $\sim$ 95.596 nm in high, respectively, while mouse plasma alone gives no any comparable nanoparticles, suggesting that the nanoparticles of NDCO-RGDS can be stably delivered in blood circulation.

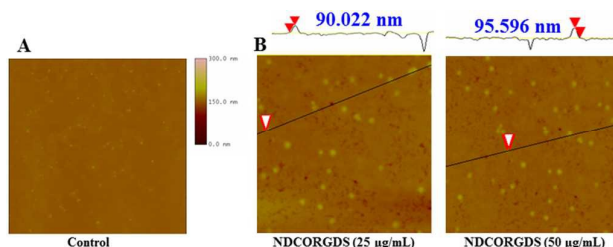


Fig. 4. AFM images. A) AFM images of mouse plasma alone; B) AFM images of 25  $\mu$ g/mL and 50  $\mu$ g/mL of NDCO-RGDS in mouse plasma.

The nano-property of the solutions of ND, NDCO<sub>2</sub>H and NDCO-RGDS in ultrapure water was identified with 650 nm laser beam induced Faraday-Tyndall effect and is shown in Fig. 5. In ultrapure water 650 nm laser beam induces 25  $\mu$ g/mL and 50  $\mu$ g/mL of them to occur Faraday-Tyndall effect (Fig. 5B - 5D). The nano-property of the solutions of ND, NDCO<sub>2</sub>H and NDCO-RGDS in ultrapure water was also characterized with the size distribution, which was

tested on a Malvern's Zetasizer (Nano-ZS90; Malvern Instruments) with the DTS (Nano) Program. Fig. 5E-5G indicates that the size distributions are 84.1 nm, 85.6 nm and 89.5 nm, respectively. The nano-property of the solution of ND, NDCOOH and NDGO-RGDS in ultrapure water was further characterized with zeta-potential, which was tested on a Malvern's Zetasizer (Nano-ZS90; Malvern Instruments) with the DTS (Nano) Program. Fig. 5H-5J indicates that the zeta-potentials are 29.6 mv, 29.9 mv and 34.1 mv, respectively. These data support the nano-properties mentioned above.

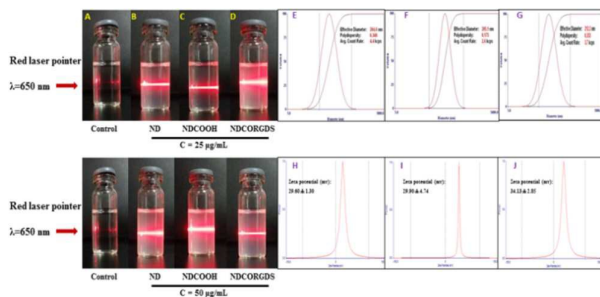


Fig.5 Nano-properties of aqueous solution, ND, NDCOOH and NDGO-RGDS.

#### NDCO-RGDS effectively carries VEGF-siRNA

The loading of VEGF-siRNA on NDCO-RGDS was analyzed with DSC,<sup>24-27</sup> and are shown in Fig.6 to describe the endothermic processes. ND and NDCO-RGDS show the endothermic peaks at ~150 °C and ~160 °C respectively. With the increase of the loading VEGF-siRNA the endothermic peak of NDCO-RGDS shifts from ~155 °C to ~145 °C. The effect of VEGF-siRNA concentration on the endothermic peak of ND and NDCO-RGDS suggests that VEGF-siRNA is effectively loaded onto NDCO-RGDS.

The loading of VEGF-siRNA was evidenced by DSC thermograms. In contrast to NDCO-RGDS, with the increase of loading VEGF-siRNA the shift of the endothermic peak of NDCO-RGDS/VEGF-siRNA ranges from ~-5 °C to ~-10 °C. VEGF-siRNA concentration dependently shifts the endothermic peak should be the result of NDCO-RGDS loading VEGF-siRNA and evidences the formation of NDCO-RGDS/VEGF-siRNA.

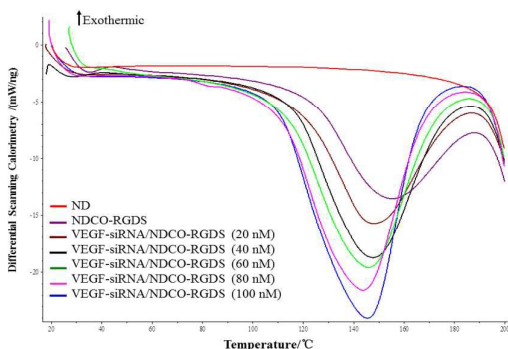


Fig.6 DSC thermograms of ND, NDCO-RGDS and NDCO-RGDS/VEGF-siRNA in 20 µL solution (DMSO: DEPC = 1:9). The samples exhibited endothermic characteristics while the concentration of VEGF-siRNA loading to NDCO-RGDS was increasing.

#### Release of RGDS and VEGF-siRNA

In TE buffer at 37 °C the release of RGDS from ND/RGDS and NDCO-RGDS was measured by ionic strength of ESI-MS. Fig. 7 shows that after aburstrelease of  $8.08 \pm 0.81\%$  a constant release of ~10.5% of the totally conjugated RGDS is monitored within 250 h. Whereas, during 75 h the RGDS linked to ND/RGDS could be completely released.

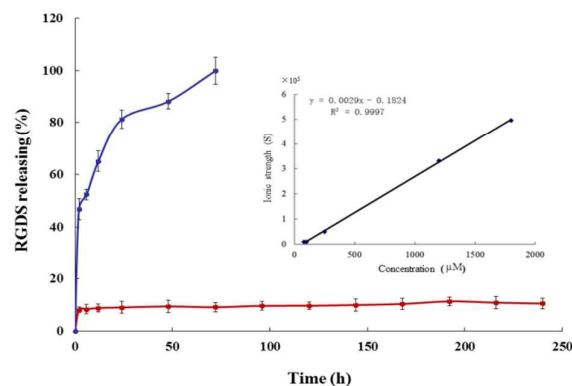


Fig.7 Release of RGDS from ND/RGDS (blue line) and NDCO-RGDS (red line). Data are presented as the average  $\pm$  SD, (n = 3).

In TE buffer at 37 °C the release of VEGF-siRNA from NDCO-RGDS/VEGF-siRNA was measured and is shown in Fig. 8. The cumulative release curves of VEGF-siRNA from NDCO-RGDS/VEGF-siRNA indicate that within 250 h VEGF-siRNA is gradually released. At 2 h,  $2.49 \pm 0.06\%$ ,  $6.23 \pm 0.94\%$  and  $7.47 \pm 0.57\%$  of VEGF-siRNA are released from  $759 \pm 82\text{ng/mg}$ ,  $1167 \pm 36\text{ng/mg}$  and  $1928 \pm 116\text{ ng/mg}$  of NDCO-RGDS/VEGF-siRNA, respectively. At 250 h,  $39.66 \pm 2.54\%$ ,  $42.22 \pm 1.36\%$  and  $49.49 \pm 2.75\%$  of VEGF-siRNA are consumed, respectively.

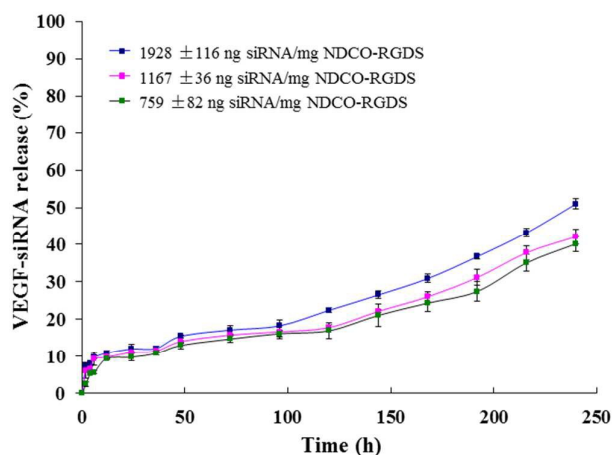


Fig.8 The releasing curves of VEGF-siRNA from NDCO-RGDS/VEGF-siRNA. Wherein the loading of VEGF-siRNA was  $1928 \pm 116\text{ ng/mg}$ ,  $1167 \pm 36\text{ ng/mg}$  and  $759 \pm 82\text{ ng/mg}$ . Data are presented as the average  $\pm$  SD, (n = 5).

In contrast to our previous ND/RGDS,<sup>19</sup> which can completely release RGDS within 50 h, within 240 h NDCO-RGDS can release only 10.52% RGDS. These results suggest that NDCO-RGDS, i.e. RGDS covalently modified NDCO<sub>2</sub>H, is stable enough as a long-circulation carrier of siRNA. The cumulative release curves of VEGF-siRNA from 3 kinds of NDCO-RGDS/VEGF-siRNA indicate that ~40% - ~50% of VEGF-siRNA can be gradually released within 250 h and show a slow release profile. Due to the siRNA of cytoplasm been easy degraded and devitalized by RNase,<sup>29,30</sup> NDCO-RGDS/VEGF-siRNA slowly release VEGF-siRNA should benefit the gene silent therapy.

#### Internalization of NDCO-RGDS/VEGF-siRNA

To test siRNA internalization HeLa cells were transfected for 6 h and observed under confocal microscope (LEICATCS SP5, Germany) to capture images. Confocal images of Fig. 9 indicate that of the control, VEGF-siRNA VEGF-siRNA/ND/RGDS and NDCO-RGDS/VEGF-siRNA treated cells only the latter can enter and consequently release VEGF-siRNA inside the cells (see the green fluorescence of figure 9D).

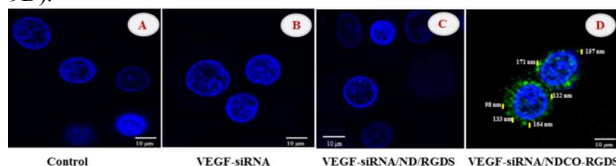


Fig.9 Confocal image of the treated HeLa cells. (A) Control; (B) VEGF-siRNA treated cells; (C) VEGF-siRNA/ND/RGDS treated cells; (D) NDCO-RGDS/VEGF-siRNA treated cells. The bright green fluorescence is NDCO-RGDS/VEGF-siRNA transferred VEGF-siRNA.

It is rational that the transfection ability of the nanoparticles of NDCO-RGDS/VEGF-siRNA for the expression inhibition of mRNA and protein of the treated cells is essential. In contrast to NDCO<sub>2</sub>H and VEGF-siRNA, the confocal images evidence that within 6 h the nanoparticles of NDCO-RGDS/VEGF-siRNA can effectively enter the cytoplasm of HeLa cells. This property ensures the transfection ability, good cytoplasm accumulation and desirable gene silencing efficacy of NDCO-RGDS/siRNA.

#### NDCO-RGDS/VEGF-siRNA inhibits the expression of VEGF mRNA *in vitro*

The transfection of VEGF-siRNA into HeLa cells by NDCO-RGDS/VEGF-siRNA was evaluated with RT-PCR, while NC/Lipo<sup>TM</sup>2000, ND/RGDS/VEGF-siRNA and VEGF-siRNA/Lipo<sup>TM</sup>2000 were used as the negative and positive controls, respectively. As shown in Fig.10, VEGF mRNA expression did not change significantly by treatment with the naked VEGF-siRNA, NC/Lipo<sup>TM</sup>2000, and NC/NDCO-RGDS as comparable to that of vehicle. Of ten agents, VEGF-siRNA/ND/RGDS and VEGF-siRNA/Lipo<sup>TM</sup>2000 equally exhibited the highest inhibiting efficiency, but significantly lower than NDCO-RGDS/VEGF-siRNA. The results indicate that 60 nM of NDCO-RGDS/VEGF-siRNA and 80 nM of VEGF-siRNA/Lipo<sup>TM</sup>2000 equally exhibit the expression of VEGF-mRNA, and the inhibition of the former shows a concentration-dependent manner. Thus RT-PCR evaluation supports NDCO-RGDS/VEGF-siRNA concentration dependently silencing VEGF of HeLa cells.<sup>29</sup>

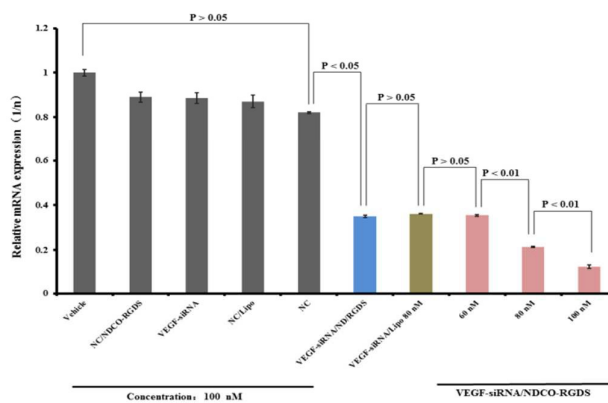


Fig. 10 VEGF mRNA expression of NDCO-RGDS/VEGF-siRNA nanoparticles treated HeLa cells. Data are presented as the average  $\pm$  SD%, (n = 3)

#### NDCO-RGDS/VEGF-siRNA silences the expression of VEGF gene *in vitro*

The efficiency of NDCO-RGDS/VEGF-siRNA silencing the expression of VEGF genes represented with the protein expression. As shown in Fig.11, the VEGF protein had the greatest inhibition treated by NDCO-RGDS/VEGF-siRNA, with a  $37.22 \pm 0.15\%$  remain in VEGF protein. It had a significant lower inhibitory effect compared to the Lipo<sup>TM</sup>2000 ( $66.05 \pm 3.05\%$ ) and ND/RGDS/VEGF-siRNA ( $49.26 \pm 2.25\%$ ) on VEGF expression. Fig. 8 indicates that 60 nM of NDCO-RGDS/VEGF-siRNA and 80 nM of VEGF-siRNA/Lipo<sup>TM</sup>2000 equally exhibit the protein expression, and the inhibition of the former shows concentration-dependent manner. Thus ELISA experiment indicates that NDCO-RGDS/VEGF-siRNA can effectively suppress the treated HeLa cells to secrete VEGF. Therefore both expressions of VEGF mRNA and secretion of VEGF protein support NDCO-RGDS/VEGF-siRNA are capable of silencing VEGF gene of HeLa cells. Moreover, the conjugating structure between ND and RGDS solved the problem of RGDS leaking from complex in the published article, and achieved in the knockdown of gene and protein.

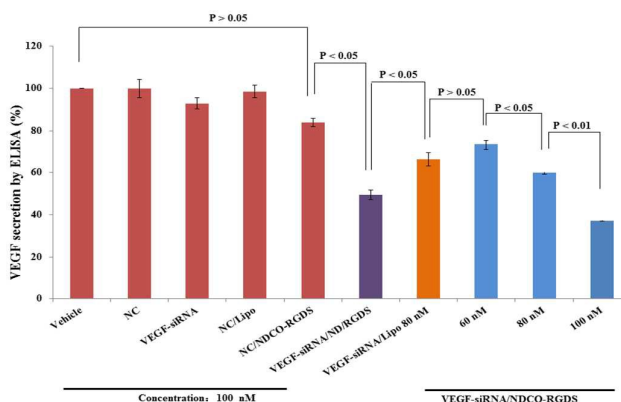


Fig.11 Protein expression of NDCO-RGDS/VEGF-siRNA treated HeLa cells. Data are presented as the average  $\pm$  SD, (n = 6).

**NDCO-RGDS/VEGF-siRNA inhibiting tumor growth of S180 mice**

The effect of NDCO-RGDS/VEGF-siRNA on tumor growth was evaluated with S180 mice. Fig.12A indicates that the tumor weights of the control and VEGF-siRNA treated mice are equal ( $p>0.05$ ), but significantly higher than that of NDCO-RGDS/VEGF-siRNA treated mice ( $p<0.01$ ). This means that by silencing the expression of VEGF gene NDCO-RGDS/VEGF-siRNA exhibits *in vivo* anti-tumor action. Similarly Fig.12B indicates that the tumor volumes of the control and VEGF-siRNA treated mice are equal ( $p>0.05$ ), but significantly larger than that of NDCO-RGDS/VEGF-siRNA treated mice ( $p<0.01$ ). This means that by silencing the expression of VEGF gene NDCO-RGDS/VEGF-siRNA slows the tumor growth *in vivo*.

Due to both NDCO<sub>2</sub>H and VEGF-siRNA exhibiting no action to the tumor growth of the S180 mice, the *in vivo* anti-tumor action of NDCO-RGDS/VEGF-siRNA on S180 mice should be the result of it releasing VEGF-siRNA into the S180 cells and consequently silencing the gene of S180 cells.

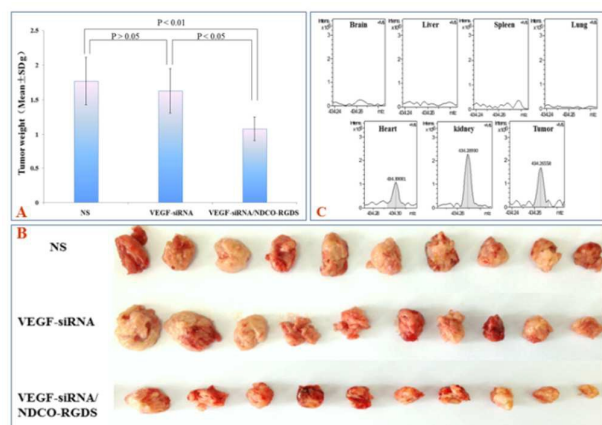


Fig.12 *In vivo* anti-tumor activity of NDCO-RGDS/VEGF-siRNA and distribution investigation. (A) Tumor weight; (B) Tumor volume; (C) FT-MS spectra based distribution; (n=10).

***In vivo* distribution of NDCO-RGDS/VEGF-siRNA**

To estimate tumor target the extracts of the organs and the tumor tissue of NDCO-RGDS/VEGF-siRNA treated mice received FT-MS examination and the spectra are shown in Fig.12C. The FT-MS spectra indicate that in the extracts of the brain, liver, spleen and lung no RGDS related peak is found, suggesting no NDCO-RGDS/VEGF-siRNA nanoparticles enter these organs. On the other hand, the FT-MS spectra indicate that in the extracts of the heart, kidney and tumor the peak of RGDS is at 434.26558-434.30081. The intensity of RGDS in the extract of tumor tissue is 1.5 folds higher than that in the extract of heart. These spectra suggest that comparing to brain, liver, spleen and lung NDCO-RGDS/VEGF-siRNA more preferentially enter the tumor tissue. On the other hand, the intensity of RGDS in the extract of kidney is 1.3 folds higher than that in the extract of tumor tissue. This comparison suggests that NDCO-RGDS/VEGF-siRNA is likely to excrete via kidney.

**NDCO-RGDS/VEGF-siRNA has no cytotoxicity**

To evaluate the cytotoxicity of NDCO-RGDS/VEGF-siRNA the MTT assay of HeLa cells was performed. Fig. 13 indicates that all reagents do not exhibit the proliferation of the cells. Non-cytotoxic siRNA carriers are of importance.<sup>31</sup> However, the nanoparticles with positive charge usually have cytotoxic effects due to the electrostatic interactions of them with negatively charged glycocalyx on cell membrane.<sup>32</sup> In the MTT assay the proliferation of the treated HeLa cells was not inhibited by NDCO-RGDS/VEGF-siRNA. This means that NDCO-RGDS/VEGF-siRNA effectively silences VEGF gene, but has no cytotoxic action.

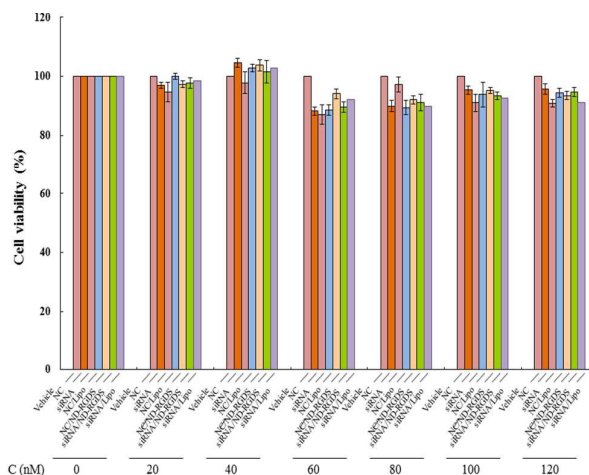


Fig. 13 Cytotoxicity assay using MTT method. Data are presented as the average  $\pm$  SD, (n=5).

**Conclusions**

A system toward gene therapy consisted of NDCO-RGDS and VEGF-siRNA, i.e. NDCO-RGDS/VEGF-siRNA, is established. The results of the *in vitro* and *in vivo* of NDCO-RGDS/VEGF-siRNA consistently support that NDCO-RGDS, as a nano-carrier, is a safe and effective vector for VEGF-siRNA delivery. As nano-particles having  $112.2 \pm 3.42$  nm of diameter and fine surfaces NDCO-RGDS/VEGF-siRNA shows the behaviour of slowly releasing and effectively transferring VEGF-siRNA over a long term. VEGF gene silencing could be induced by NDCO-RGDS/VEGF-siRNA without showing cytotoxicity.

**Acknowledgements**

This work was supported by Beijing Municipal Science & Technology Commission (Z141100002114049), PXM2013-014226 000002, TJSHG (201310025008), IHLB (KZ20121-0025021), National Natural Science Foundation (81172930, 81273379, 81373264, 81373265, 81270046 and 81502688), Joint Research and Development of protective agents for low dose radiation injury (2014DFR30930), the Importation and Development of High-Caliber Talents Project of Beijing

Municipal Institutions, Natural Science Foundation of Capital Medical University (2015ZR14) and China's 55 of postdoctoral scientific research funds.

## Notes and references

- ME. Davis, *et al.*, Evidence of RNAi in humans from systemically administered siRNA via targeted nanoparticles, *Nature*, 2010, 464, 1067-1070.
- HM. Aliabadi, B. Landry, C. Sun, T. Tang and H. Uludağ, Supramolecular assemblies in functional siRNA delivery: where do we stand? *Biomaterials*, 2012, 33, 2546-2569.
- Rafael G. Mendes, Alicja Bachmatiuk, Bernd Büchner, Gianaurelio Cuniberti and Mark H. Rummeli, Carbon nanostructures as multi-functional drug delivery platforms, *J. Mater. Chem. B.*, 2013, 401-428.
- X. Liu, *et al.*, The influence of polymeric properties on chitosan/siRNA nanoparticle formulation and gene silencing, *Biomaterials*, 2007, 28, 1280-1288.
- CM. Kummitha, AS. Malamas and ZR. Lu, Albumin pre-coating enhances intracellular siRNA delivery of multifunctional amphiphile/siRNA nanoparticles, *Int J Nanomedicine*, 2012, 7, 5205-5214.
- Jianfeng Guo, Karen A. Fisher, Raphael Darcy, John F. Cryan and Cairiona O'Driscoll, Therapeutic targeting in the silent era: advances in non-viral siRNA delivery, *Mol. BioSyst.*, 2010, 6, 1143-1161.
- Andrzej Gallas, Cameron Alexander, Martyn C. Davies, Sanyogita Puri and Stephanie Allen, Chemistry and formulations for siRNA therapeutics, *Chem. Soc. Rev.*, 2013, 42, 7983-7997.
- Anke Krüger, Yuejiang Liang, Gerald Jarre and Jochen Stegk, Surface functionalisation of detonation diamond suitable for biological applications, *J. Mater. Chem.*, 2006, 16, 2322-2328.
- Yingqi Li, Xueping Zhou, Dongxin Wang, Binsheng Yang and Pin Yang, Nanodiamond mediated delivery of chemotherapeutic drugs, *J. Mater. Chem.*, 2011, 21, 16406-16412.
- B. Moosa, K. Fhayli, S. Li, K. Julfakyan, A. Ezzeddine and NM. Khashab, Applications of nanodiamonds in drug delivery and catalysis, *J. Nanosci Nanotechnol.*, 2014, 14, 332-343.
- VN. Mochalin, O. Shenderova, D. Ho and Y. Gogotsi, The properties and applications of nanodiamonds, *Nat Nanotechnol.*, 2011, 7, 11-23.
- A. Alhaddad, *et al.*, Nanodiamond as a vector for siRNA delivery to Ewing sarcoma cells, *Small.*, 2011, 4, 3087-3095.
- J. Li, Y. Zhu, W. Li, X. Zhang, Y. Peng and Q. Huang, Nanodiamonds as intracellular transporters of chemotherapeutic drug, *Biomaterials*, 2010, 31, 8410-8418.
- R. A. Shimkunas, *et al.*, Nanodiamond-insulin complexes as pH-dependent protein delivery vehicles, *Biomaterials*, 2009, 30, 5720-5728.
- H. Kim, *et al.*, Multiscale simulation as a framework for the enhanced design of nanodiamond-polyethyleneimine-based gene delivery, *J. Phys. Chem. Lett.*, 2012, 3, 3791-3797.
- JR. Bertrand, *et al.*, Plasma hydrogenated cationic detonation nanodiamonds efficiently deliver to human cells in culture functional siRNA targeting the Ewing sarcoma junction oncogene, *Biomaterials*, 2015, 45, 93-8.
- M. Mkandawire, *et al.*, Selective targeting of green fluorescent nanodiamond conjugates to mitochondria in HeLa cells, *Biophotonics.*, 2009, 2, 596-606.
- C. Nazli, TI. Ergenc, Y. Yar, HY. Acar and S. Kizilel, RGDS-functionalized polyethylene glycol hydrogel-coated magnetic iron oxide nanoparticles enhance specific intracellular uptake by HeLa cells, *Int J Nanomedicine.*, 2012, 7, 1903-1920.
- Chunying Cui, *et al.*, Preparation and Characterization of RGDS/Nanodiamond as a Vector for VEGF-siRNA Delivery, *J. Biomed. Nanotechnol.*, 2015, 11, 70-80.
- R. Kaur, *et al.*, Lysine-functionalized nanodiamonds: synthesis, physicochemical characterization, and nucleic acid binding studies, *Int J Nanomedicine.*, 2012, 7, 3851-66.
- XQ. Zhang, *et al.*, Polymer-functionalized nanodiamond platforms as vehicles for gene delivery, *ACS Nano.*, 2009, 22, 2609-2616.
- H. Huang, E. Pierstorff, E. Osawa and D. Ho, Protein-mediated assembly of nanodiamond hydrogels into a biocompatible and biofunctional multilayer nanofilm, *ACS Nano.*, 2008, 2, 203-212.
- K. Park, MY. Lee, KS. Kim and SK. Hahn, Target specific tumor treatment by VEGF siRNA complexed with reducible polyethyleneimine-hyaluronic acid conjugate, *Biomaterials*, 2010, 31, 5258-5265.
- K. Ladewig, M. Niebert, ZP. Xu, PP. Gray and GQ. Lu, Efficient siRNA delivery to mammalian cells using layered double hydroxide nanoparticles, *Biomaterials*, 2010, 31, 1821-1829.
- N. Murata, Y. Takashima, K. Toyoshima, M. Yamamoto and H. Okada, Anti-tumor effects of anti-VEGF siRNA encapsulated with PLGA microspheres in mice, *J Control Release.*, 2008, 20, 246-254.
- CW. Lu, Q. Wang, YX. Chen and JL. Shi, Simultaneous characterizing study of the metallic ironorganic coordination compound ND by TG-DSC-MS coupling techniques, *Thermochimica Acta.*, 2003, 404, 63-70.
- Ficarra R, Ficarra P, Di Bella MR, Raneri D, Tommasini S, Calabrò ML, *et al.* Study of beta-blockers/beta-cyclodextrins inclusion complex by NMR, DSC, X-ray and SEM investigation, *J Pharm Biomed Anal.*, 2000, 23, 33-40.
- CP. Lin, YM. Chang, JP. Gupta and CM. Shu, Comparisons of TGA and DSC approaches to evaluate nitrocellulose thermal degradation energy and stabilizer efficiencies, *Process Safety and Environmental Protection.*, 2010, 88, 413-419.
- E. Smid and J. Tintner, Application of differential scanning calorimetry (DSC) to evaluate the quality of compost organic matter, *Thermochimica Acta.*, 2007, 459, 87-93.
- D. Cun, DK. Jensen, Maltesen MJ, Bunker M, Whiteside P, Scurr D, *et al.* High loading efficiency and sustained release of siRNA encapsulated in PLGA nanoparticles: quality by design optimization and characterization, *Eur J Pharm Biopharm.*, 2011, 77, 26-35.
- Atsushi Tamura, Nobuhiko Yui. A supramolecular endosomal escape approach for enhancing gene silencing of siRNA using acid-degradable cationic polyrotaxanes, *J. Mater. Chem. B.*, 2013, 1, 3535-3544.
- Li J, Zhu Y, Li W, Zhang X, Peng Y, Huang Q. Nanodiamonds as intracellular transporters of chemotherapeutic drug, *Biomaterials*, 2010, 31, 8410-8418.